Influence of Geometric Parameters on Inlet-losses during the Filling Process of Screw-Type Motors

Univ. Prof. Dr.-Ing. Andreas Brümmer, Dipl.-Ing. Jan Hütker

Technische Universität Dortmund, Fakultät Maschinenbau, Fachgebiet Fluidtechnik,
Leonhard-Euler-Str. 5, 44227 Dortmund, Deutschland
e-mail: fluidtechnik.mb@tu-dortmund.de

Keywords: steam-powered screw motor, screw machine, screw motor, screw engine

1. Introduction

In applications as an expansion motor for steam-type working fluids, the screw machine is mainly used for decentralised energy systems in the low to medium performance range. In applications of this kind, the high efficiency and good performance under part-load conditions over a wide load-range are responsible for the energetic advantages of the screw motor compared with alternative types of machine. The functional characteristics of the screw motor allow the expansion of steam in all its various forms, from super-heated steam to saturated steam [1]. This opens up operating areas for the screw motor which are beyond the scope of turbines.

In this article, a geometric steam-powered screw motor design for a specific application will be described using a chamber model, and the results relating to geometrical influences on motor behaviour will be discussed. The design of a screw machine to be deployed as a steam expander differs from the development of a compressor from both the energy point aspect and the construction principles. The systematic variation of the geometric parameters of the internal volumetric ratios, the length-diameter ratio and the wrap angles, combined with an examination of the effects on machine performance, provide basic information about the mechanisms which lead to loss of efficiency in the machine. These losses can mainly be put down to choke effects and gap losses during the filling process. Finally, the influence of parameter variation on the performance of the steam-powered screw motor will be demonstrated by showing the extent to which efficiency rating and internal performance depend on the geometrical machine parameters.

2. Screw Motor design

Working principle

In general, screw machines belong to the displacement machine group, and, within this group, to the double-shafted rotary cylinder type with internal compression [2]. If there is an external energy input in order to increase the energy content of the working medium, one refers to a screw compressor. In the opposite case, the compressed and heated fluid applies force to the rotor flanks of the machine, and, according to the definition, we are dealing with a screw motor (**Fig. 1**).

Fig. 1: Sectional representation of a screw-type motor

The operating principle of the screw motor is based on the screw-shaped, spiral intermeshing rotors, which rotate in opposite directions inside a close-fitting housing. The tooth gaps of the rotors, in combination with the housing, form the working chambers. When the rotors in a displacement machine turn, typical cyclical changes in the volume of the working chambers take place. Several operating cycles take place sequentially, during which the working chambers on the high pressure side are continually enlarged during the charging phase, while those on the low pressure side reduce in size as they are emptied. Via apertures in the housing, connections between the working chambers and the inlet and outlet ports are created, according to the rotation angle of the rotors. The chambers are normally enclosed except for the rotor clearances. The rims of these apertures, those which close off the charging phase and open for the discharge phase, are referred to as control edges. The rotation angle positions of the control edges determine the internal volume changes in the working chambers.

In displacement machines, there is always an important functional separation of moving and stationary parts. The relative movement between the rotors and the internal surfaces of the housing inevitably results in gaps, which prevent mechanical friction between the rotors, and also between the rotors and the housing. There are various ways in which the gaps influence the operational efficiency and security of the machine. They are responsible for connections between the individual working areas.

and between the working chambers on the low and high pressure sides of the machine respectively. The rotor geometry determines the length and form of the gaps [3].

Volume curve and inlet area

The volume curve represents the volumetric progression of the working chamber depending on the rotation angle of the male rotor. In the zero position of the male rotor the volume of the working chamber under examination is also zero (**Fig.2**). The volume curve characteristically shows a continuous slope up to the point where full profile intermeshing has taken place, followed by a linear progression, and a diminishing rise up to the point where maximum chamber volume is reached.

The inlet area, which depends on the rotation angle, is the cross-section area which is available for the working fluid to flow through during the charging phase. This area is formed by the apertures in the housing and the rotor teeth, which circulate past these gaps, covering and uncovering parts of them. The inlet area can be represented as a function of the male rotor rotation angle, analogous to the volume curve. Depending on the profile, the development of the inlet area frequently begins at a rotation angle differing from the zero position of the male rotor. The reason for this is a tooth gap area opening at the front face, which runs ahead of the actual working chamber, and is connected to the low pressure side [2]. The inlet area progression ends with arrival at the control edges, at the rotational angle which indicates the theoretical start of expansion.

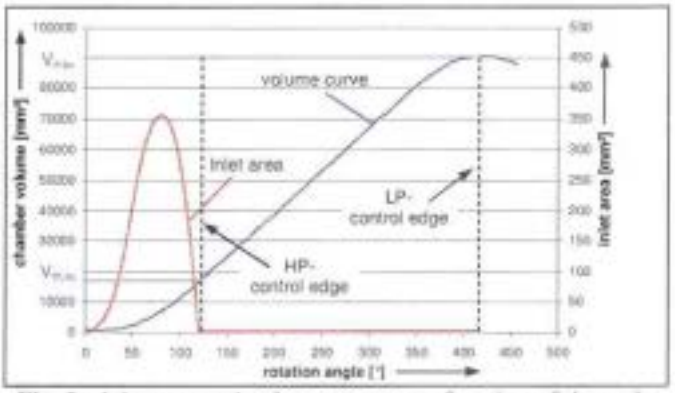

Fig. 2: Inlet area and volume curve as a function of the male rotor rotation angle on a typical steam-powered screw motor

Working cycle of a screw motor

In principle, a working cycle includes all processes in the working area, beginning at a particular thermodynamic state and ending at the next occurrence of the same state. The working cycle of a screw motor consists of three characteristic phases: charging of the working chamber, expansion phase, and discharge of the working fluid.

During the charging phase, the port on the high pressure side is charged with the working fluid at high temperature and pressure, so that the medium flows into the tooth gap behind it through the inlet area. As the rotor continues to turn, the chamber volume grows. The charging phase ends when the working chamber no longer has any connection with the inlet aperture on the high pressure side (**Fig. 3**). As the area of the inlet port is small at the beginning of the cycle, resulting in a high choking effect, maximum chamber pressure is not achieved immediately, but is reached as the rotor moves on. This difference during the charging phase between the initial pressure and the maximum pressure in the chamber is characteristic for the charging phase. This difference is the result of pressure loss caused by choking as the fluid flows in, and gap losses from the working chamber. A further aspect of the real-life charging process is that expansion begins before the control edge on the high pressure side has been reached. The pressure gradient at the end of the charging process is already comparable with that during the first expansion phase beginning at, when the control edges have been reached. The reason for the early start of expansion is essentially a combination of continuously rising chamber volume combined with reducing area at the inlet port. The point at which expansion actually starts is inherent in the system, and also occurs in an ideal scenario where choke effects and gap losses are ignored.

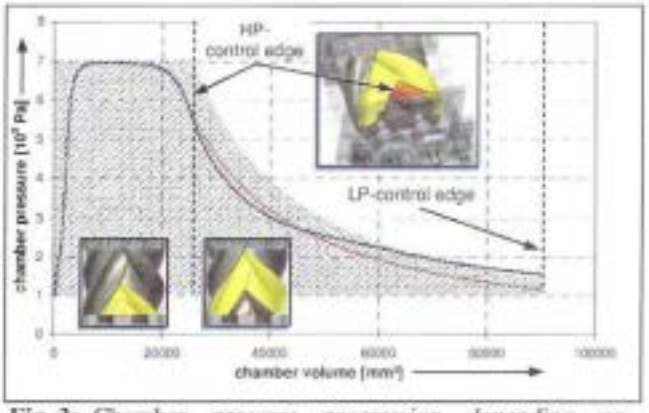

Fig. 3: Chamber pressure progression depending on chamber volume with
- real and
- isentropic expansion phases

At the start of the expansion phase, the operating behaviour of the screw motor is mainly influenced by gap flows. In order to assess the effect of gap flows on the energy conversion rating of the motor, a distinction has to be made between loss flows out of the working chamber under examination and flows into the chamber through other gap interconnections. Compared with isentropic expansion, the actual pressure progression during initial expansion rises more steeply in the theoretical representation. The reason for this is that the fluid losses from the chamber are proportionally higher than the gains. As rotation continues, real and isentropic chamber pressures converge, until, in the second phase of expansion, pressures during the real process exceed those for the isentropic expansion process. The more gradual pressure progression during the real process is a consequence of flows into the working chamber from those following it. This fluid does not flow directly into the low-pressure side of the motor, but helps to some extent to fill the expanding chamber under consideration, applying power to the rotor

flanks. The expansion phase ends when maximum chamber volume has been achieved. As a rule, at this point in the cycle the leading tooth flanks pass across the control edges at the low pressure side, and pressure equalisation takes place (represented isochorically in Fig. 3).

The discharge progress is represented in the following in idealised form by means of isochoric pressure equalisation between the chamber pressure and the low pressure machine pressure as the low pressure side control edges are passed. In the following description of the effects of varying final expansion pressures, a model will be used which utilises an isobaric charge, followed by isentropic expansion restricted by constant fluid mass in the working chamber (**Fig. 4**).

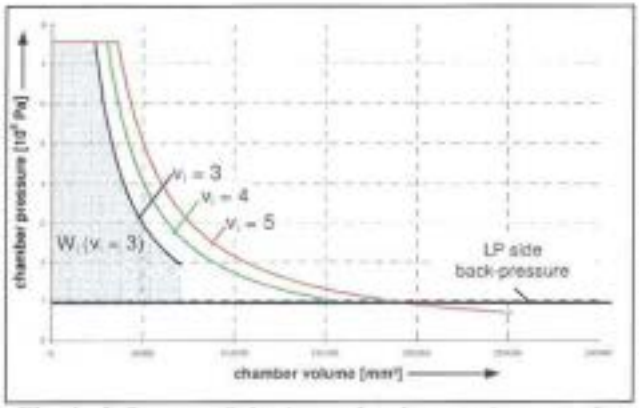

Fig. 4: Influence of the internal volume ratio v_i on the working area W_i under constant machine conditions.

If there is no difference between the chamber pressure at the end of the expansion phase and the ambient machine pressure on the low pressure side, this is known as 'aligned operation'. When the selected inner volume ration is too high see $v_i = 5$, the chamber pressure falls below the low pressure side ambient pressure during the expansion phase. The 'over-expanded' fluid mass will be isochorically compressed (in idealised form) by working fluid flowing back through the low-pressure port before it can be expelled. As soon as the chamber pressure falls below the ambient machine pressure of the low pressure side, the effective work performed by the fluid during the expansion phase is more than counterbalanced by the additional work required to expel it. During this phase, the steam-powered screw motor functions as a compressor. On the other hand, if the selected internal pressure ration is too low, chamber pressure at the end of the expansion phase is higher than ambient machine pressure on the low-pressure side, resulting in continuing isochoric expansion (in idealised form) of the working fluid as it passes the control edges on the low pressure side. Part of the theoretically available energy in the fluid thus remains unused because of the too-short expansion phase.

3. Theoretical foundations

In order to assess the energy conversion rating of screw motors with varying geometrical parameters, operating values and boundary conditions must be laid down, within which the different motor variations are comparable. Although the functioning of a screw motor is more or less like that of a screw compressor working the other way round, both the definition of the boundary conditions and the physical description of the processes in the working areas are more complex than in the case of screw compressors. In the following, operating values will be defined and applied, which allow both an assessment of varying rotor geometries and the energetic examination of differing motor variants.

Geometrical operating values

In the next section the operating values for the gap situation and the configuration of the inlet area will be defined, so that an assessment of these elements can be quantified. In contrast to the throughput ratio and charging ratio, both sets of operating values refer here to the geometrical characteristics of the screw motor, and are independent of any energetic examination of the working cycle.

The gap value sets the fluid mass $m_{g,fill}$ in relation to the theoretical fluid mass $m_{th,ex}$ at the start of the expansion phase at high pressure control edge:

$$\Pi_g = \frac{m_{g,fill}}{m_{th,ex}} \qquad \text{(Eq. 1)}$$

The fluid mass $m_{g,fill}$ is the mass which, in the rotation angle area for charging between α_{start} and $\alpha_{th,ex}$, flows out of the working chamber through the time-dependent gap area of the chamber to be charged $A_g(t)$. For the gap flow, a supercritical decompression at the speed of sound in the narrowest cross-section is assumed:

$$\Pi_g = \frac{\int_{\alpha_{start}}^{\alpha_{th,ex}} A_g(t)\,dt \cdot \left(\frac{2}{\kappa_e+1}\right)^{\frac{1}{\kappa_e-1}} \cdot \frac{p_e}{R \cdot T_e}\sqrt{\frac{2\cdot\kappa_e}{\kappa_e+1}\cdot R \cdot T_e}}{V_{th,ex}\cdot \rho_e} \qquad \text{(Eq. 2)}$$

The computation is based on the model of a stationary and isentropic gap flow through the narrowest cross-section, with

negligible flow speed before entrance. According to the assumption of a blocked flow which has been adopted in this case, the leakage value is a function of the initial parameters (temperature and pressure) and the time factor (r.p.m.), and a function of the gap area, which depends in its turn on geometry and time.

Small gap values are responsible for a favourable gap situation and small gap flows during the charging process. Leakages through machine gaps during the compression phase do contribute to a loss of fluid mass, but the chamber is 'topped up' by an inflow from the following chambers in a kind of recovery process. Restricting the examination to the rotation angle area of the charging process can therefore be justified by the exclusively dissipative character of the gap flows during this phase of the cycle.

The inlet area value sets the mean fictitious inward flow speed $\bar{c}_{e,f}$ in relation to the speed of sound $a_e = f(p_e, T_e)$:

$$\Pi_{in} = 1 - \frac{\bar{c}_{e,f}}{a_e} = 1 - \frac{\overline{\left(\frac{\Delta V_c(t)}{A_{in}(t)}\right)}}{a_e} \qquad \text{(Eq. 3)}$$

The fictitious inward flow speed as already employed by Huster [5] is calculated from the time-step related quotients arising from changes to the chamber volume ΔV_c (t) and inlet area A_{in} (t). The inlet area value depends only on the geometry and the inflow parameters, analogous to the gap value. It would be worth developing a motor with a larger inlet area value, as this would result in a longer charging phase and a larger inlet area.

Modelling and computation

The variation calculations were carried out in two independent steps: geometrical abstraction and energetic examination. The basis for geometrical abstraction of the screw motor is the analytical treatment of the rotor gear teeth [5]. The aim of this calculation is to determine the volume curve, the dimensions of the inlet and outlet areas, and the gap areas as a function of the male rotor angle at a specified geometrical parameter (z_{MR}, z_{FR}, φ_{MR}, L/D und v_i). The results of the geometrical abstraction form the basis for the energetic examination of the operational behaviour of the motor.

The computation program for an energetic machine analysis is generally based on mass and energy conservation. Basically, by means of a balancing process, changes in the condition of the working fluid (steam) are established numerically, so that the operating behaviour of the machine can be represented. Variations in the form of volume changes depending on rotation angle changes and gap flows in and out of the working chamber are taken into account. The computational basis for the progression the condition of the working fluid represents, in view of the flow speed, a zero-dimensional chamber model, which makes it possible in principle to simulate screw motors with random geometrical parameters.

4. Investigation of the influence of geometric parameters on the operating performance of Screw Motors

Operating and boundary conditions

The investigation of the operating behaviour of screw motors by the use of thermodynamic simulation is the basis for the subsequent experimental research of the machine. In order to carry out a geometrical comparison of different machines, it is first necessary to lay down the boundary conditions under which the machines are comparable. In the present case, the parameter combination of inflow pressure p_e, inflow temperature ϑ_e, and theoretically transportable mass flow $\dot{m}_{th}$ was laid down for the external boundary conditions of the screw motor. Although variation options are possible over a broad, technically feasible area, setting the initial conditions was not done on a random basis, but based on installation conditions like those which can be found in industrial applications with small mass flows.

- working medium: water steam
- inflow pressure $p_e = 7 \cdot 10^5$ Pa
- inflow temperature $\vartheta_e = 350$ °C
- theoretical mass flow $\dot{m}_{th} = 0.1$ kg·s^{-1}

The theoretical mass flow is used instead of the ambient machine mass flow as a reference value, because it depends only on the known machine geometry and the rotor speed, but not on the motor operating values. The theoretical mass flow is calculated as the product of the chamber volume at the start of expansion $V_{th,ex}$, and the density ρ_e as a function of the values at the entry port, the tooth count z_{MR} and the rotor revolutions n_{MR}:

$$\dot{m}_{th} = V_{th,ex} \cdot \rho_e \cdot z_{MR} \cdot n_{MR} = \frac{V_{min}}{v_i} \cdot \rho_e \cdot z_{MR} \cdot n_{MR}$$

(Eq. 4)

Initially, the working range of the screw motor is limited, according to the Clausius-Rankine-Cycle, entirely to the superheated area in the parameter combination dealt with here. The entry parameters do not allow any transfer phases caused by entering the saturated steam range to occur during the expansion phase, even under isentropic process management.

Along with constant machine parameters, additional border conditions for the screw motor are defined. These conditions are set by the speed of the rotor crown circle and the mean gap clearance. For variations in the rotor geometry, the male rotor circumference speed is defined as $u_{MR} = 100\ m \cdot s^{-1}$. This value has a major influence on the energy conversion rating of the machine, and corresponds to 30 000 r.p.m with a male rotor diameter of 65 mm. All gap heights are treated as constant at $h_s = 0.2$ mm. This assumption is justified by the fact that gap heights do not vary significantly in different-sized machines. Geometrical variations as a result of thermal interaction between the working fluid and the housing or the rotors respectively are not taken into account, and could provide potential for further studies.

Variation calculations

The configuration of geometrical parameters for screw motors presented below incorporates variations in internal volumetric relations, wrap angle and length-diameter relations. As a starting point for the variation calculations a combination of four male rotor teeth ($z_{MR} = 4$) and six female rotor teeth ($z_{FR} = 6$) was selected, which represents a compromise between small integral clearances and a sufficiently large rotation angle range for charging the chamber.

Variations in the internal volume ratio

The internal volume ratio does not depend on the rotor geometry, and is determined via the sitting of the control edges in the motor housing. According to the definition, the internal volume relationship of a screw motor results from the relationship between chamber volume at the end of the expansion phase V_{max} and the chamber volume at the theoretical start of expansion $V_{th,ex}$:

$$v_i = \frac{V_{max}}{V_{th,ex}} \qquad \text{(Eq. 5)}$$

When a screw machine is deployed as a motor, variation in the internal volume relationship occurs when the high pressure side control edges are re-sited. With constant geometrical rotor parameters, increasing the internal volume ratio means that the control edges have to be moved towards smaller rotor angles, which leads in its turn to a reduction of the chamber volume at the start of expansion (**Fig. 5**). As the pre-requisites for varying the internal volume are constant theoretical mass flow in combination with constant male rotor circumference speed, these requirements are significant restrictions on the size of the machine. In order to fulfil the relevant border conditions, which consist of the machine parameters, the circumference speed and the mean gap height, geometrically similar machines – even down to the $h_s = 0.2$ mm gaps - with identical geometrical parameters, were used for the energetic computation.

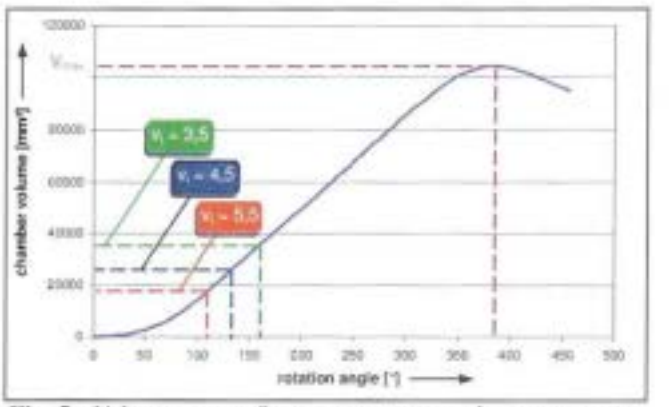

Fig. 5: Volume curve for a steam-powered screw motor with varying internal volume relationships

The chamber pressure as a function of the chamber volume is represented in **Fig. 6** for steam-powered screw motors with varying internal volume relationships. The wrap angle and the length-diameter relationship, along with the theoretical mass flow have been kept constant. The graph shows pressure progression during the charging phase, and expansion, without taking the low pressure side charge transfer into account.

For small internal volume ratios the chamber pressure progression during the charging process shows only a minor pressure difference between the entry pressure and the chamber pressure. However, this positive effect on the working area has to be set against the high expansion pressure and the resultant unused exergy. On the other hand, with large internal volume relationships, charge transfer work leads, as a result of 'over-expansion', to a reduction in internal work. These tendencies persist if the internal volume relationship is varied in combination with different wrap angles or length-diameter

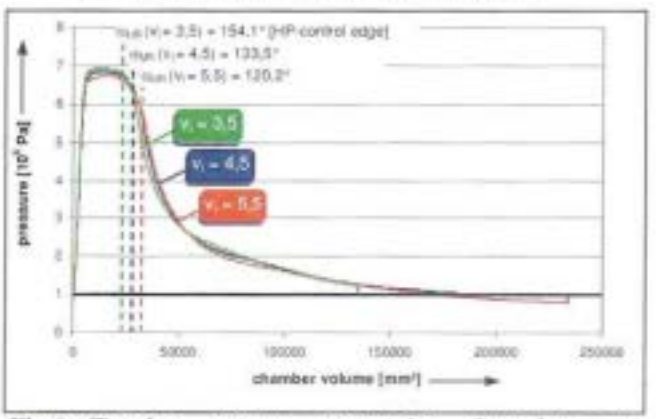

Fig 6: Chamber pressure progression dependent on chamber volume for varying internal volume relationships v_i
($z_{MR} = 4$, $z_{FR} = 6$, $\varphi_{MR} = 350°$, L/D = 1.4)

relationships respectively.

In order to assess the geometrical effects of varying the internal volume relationships, it was decided not to carry out an examination of inlet area and gap values. Although these two operating values permit quantitative statements to be made concerning the configuration of the gap characteristics and the inlet geometry during the charging phase, it would seem that, in connection with variation in internal volume relations, final expansion pressure is the really vital criterion. This is essentially a direct result of the internal volume ratio, and is only peripherally affected by dissipative processes during the charging phase.

Geometrical examination of varying wrap angles

In order to examine the influence of the wrap angles on performance, different pairs of rotors are varied in such a way that only the wrap angles are changed. The length-diameter ratio, the internal volume ratio and the theoretical mass flows of all rotor pairs remain constant. **Fig. 7** shows rotor pairs with different wrap angles, but with all other geometrical values unchanged.

Fig 7: Rotor pairs with varying wrap angles φ_{MR}

Varying the wrap angle affects both the gap situation and the geometry of the inlet area. In order to achieve a quantifiable description of the geometrical effects, an inlet area value Π_{ia} and a gap value Π_g were selected. In **Fig. 8** the dependence of both values on the male rotor wrap angle in machines with an internal volume ratio of $v_i = 4$ and a length-diameter ratio of L/D = 1.4, is represented.

In the parameter area for wrap angles from φ_{MR} = 200° - 400°, increasing wrap angles result in a rise in the inlet area value Π_{ia} - which would suggest an improvement in mass transport from the high pressure port into the working area, and lower choking losses as a result. As the wrap angle increases, both longer charging times and the larger maximum area of the inlet opening during the charging phase contribute to a rise in the performance figures (**Fig. 9**). Representing the inlet area as a time function was employed rather than as a function of the male rotor rotation angle, as this did not provide sufficient feedback because of varying rotor speeds.

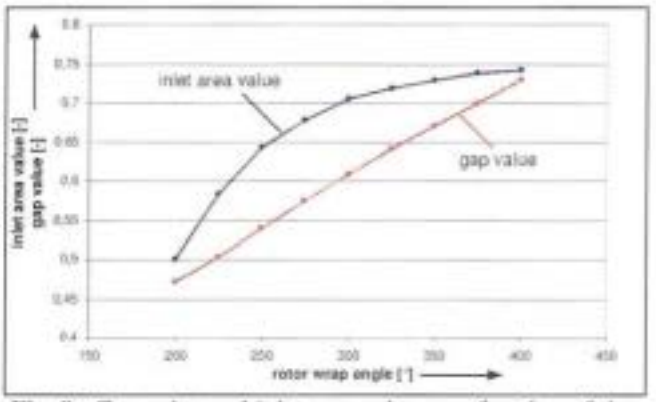

Fig. 8: Gap value and inlet area value as a function of the wrap angle
(z_{MR} = 4, z_{FR} = 6, v_i = 4, L/D = 1.4)

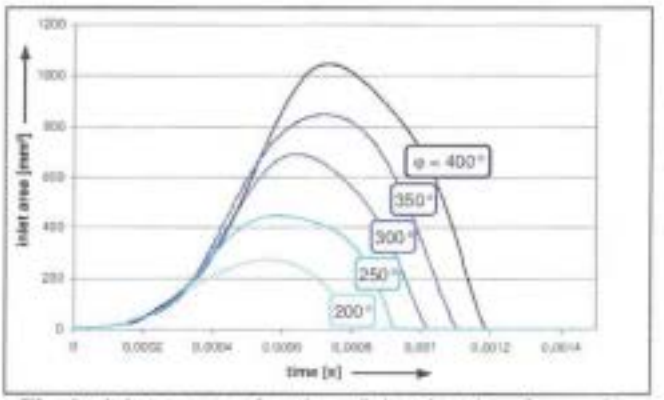

Fig. 9: Inlet area as a function of charging time for varying male rotor wrap angles
(z_{MR} = 4, z_{FR} = 6, v_i = 4, L/D = 1.4)

Raising the wrap angle at constant step angle ($\Delta\varphi$ = 50°) closely matches a continuous rise in the charging time ($\Delta t_{III} \approx 9.5\ 10^{-5}$ s) and also in the maximum size of the inlet area ($\Delta A_{ia\,max} \approx 190$ mm²). On the other hand, the degressive rise in the inlet values as a function of the wrap angle reflects the relatively smaller increase in charging time and the maximum size of the inlet area.

In contrast to the inlet area value, there is a linear rise in the gap value as the wrap angle increases. In **Fig. 10** the time-dependent gap area processes during the charging phase are represented for motors with varying wrap angles.

With a small wrap angle as a starting point, an increase in the angle leads not only to the increase in the charging time as already dealt with, but also to a rise in the integral gap area. As

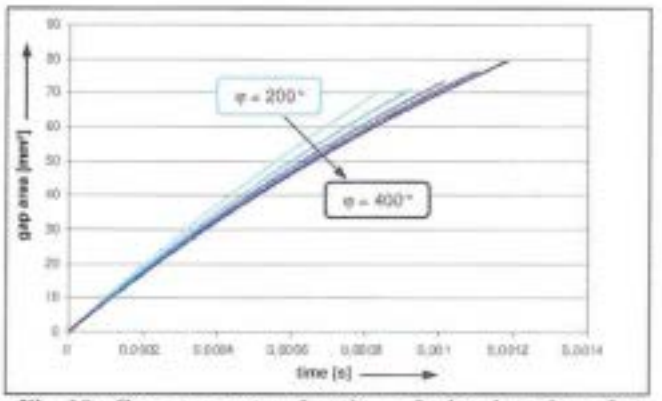

Fig. 10: Gap area as a function of charging time for varying male rotor wrap angles
(z_{MR} = 4, z_{FR} = 6, v_i = 4, L/D = 1.4)

both the charging time and the gap area are included in the computation in linear form, the gap area progression indicates a predominant influence of the charging time over the gap area. Starting with the smallest wrap angle examined $\varphi_{MR} = 200°$, a doubling of the wrap angle leads to a 43.3% longer charging time. By contrast, the maximum gap area only increases by 14.1%.

A geometrical examination of the influence of varying wrap angles on inlet and gap values shows opposing tendencies. The extent to which the favourable gap situation brought about by small wrap angles results in energetic advantages compared with the inlet area geometry aimed at with larger wrap angles, cannot be assessed on the basis of the geometrical values alone.

Energetic examination of varying wrap angles

The influence of the wrap angle on energy conversion will be further examined by means of an efficiency rating analysis and a comparison of the internal power ratings. The efficiency rating which is limited to the charging process and the expansion phase, permits a differentiated examination of the dissipative effect of gap leakages and the choke effect of the inlet area, and also throws light on the relative priority of these two principal physical loss mechanisms. Along with the inlet area and gap values, the operating efficiency and the internal power ratings also contribute to a deeper understanding of dissipative processes during the charging phase.

In order to arrive at more precise conclusions concerning the influence of geometrical variations on the energy conversion efficiency of the steam-powered screw motor, a comparative approach is useful. In an ideal process control system, the working area is characterised by isobaric charging and discharging, and isentropic expansion in a suitably aligned operation. The border conditions for calculating the actual working surface are based on the assumption of an adiabatic process in which loss mechanisms are taken into account. The difference in area compared with an ideal comparison process results from the restricted inflow of charging fluid at the beginning and end of the charging phase, from the choke effect of the inlet port area, and the gap losses. The internal efficiency factor η_i relates the working area in a real process to the ideal comparative process:

$$\eta_i = \frac{W_i}{W_{i,id}} \qquad \text{(Eq. 6)}$$

The dependence of the efficiency rating and the internal power rating on the wrap angle is shown in **Fig. 11**. With small wrap angles, efficiency is relatively low, both for the charging process in isolation, and also if expansion is taken into account. As the examination of the inlet area and gap values demonstrates, motor variants with small wrap angles are characterised by a favourable gap situation but unfavourable inlet geometry. As the wrap angle increases, both efficiency ratings rise degressively, an effect which can be explained in terms of decreasing integral dissipation. With regard to the inlet area and gap values, it is mainly improving inlet geometry as the wrap angle increases which is responsible for improved efficiency. This factor outweighs the deteriorating gap situation. The further improvement with larger wrap angles when expansion is taken into account, can be put down to gap mass flows which 'top up' the working chamber from the following chambers.

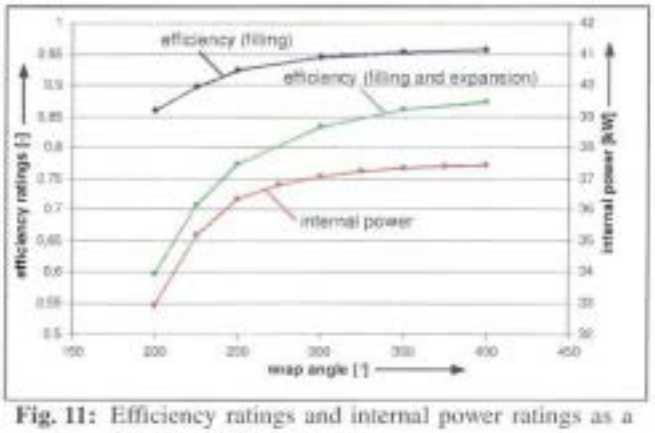

Fig. 11: Efficiency ratings and internal power ratings as a function of the wrap angle
($z_{MR} = 4$, $z_{FR} = 6$, $v_i = 4$, $L/D = 1.4$)

The internal power rating shows a trend towards a comparable dependency on the wrap angle. Although an increase in the wrap angle in the range $\varphi_{MR} = 200° - 300°$, leads at first to a significant improvement in the internal power rating, a further enlargement only leads to a minor improvement.

Geometrical examination of varying the length-diameter ratio

The length-diameter ratio L/D is the third parameter, along with the tooth count and the wrap angle, involved in describing the rotor geometry. The area of variation described below covers length-diameter ratios from L/D = 1.2 – 1.8. Rotor pairs with differing length-diameter ratios are shown in **Fig. 12**.

Fig. 12: Rotor pairs with differing length-diameter ratios

As in the case of the wrap angle, the length-diameter ratio influences both the overall gap situation and the inlet area geometry of the steam-powered screw motor. The effects of varying this ratio on the geometrical configuration of the rotors

will be assessed using the inlet area value Π_{ia} and the gap value Π_{g}. Both these figures achieve their highest values in the range of low length-diameter ratios (**Fig. 13**). As the ratio increases, the decreasing inlet area value indicates the deteriorating geometrical configuration of the inlet area, while the reducing gap value indicates a positive effect on the gap situation.

The effects of increasing length-diameter ratios on the inlet situation are qualitatively similar to those achieved by reducing the wrap angle. The maximum values for both the inlet area and the charging times rise as the length-diameter ratio falls, which accounts for the high input area values in this parameter range. On the other hand, longer charging times have a negative effect on the gap values. Along with the charging time, increasing integral gap areas contribute to a rise in these values as length-diameter ratios decrease (**Fig. 14**).

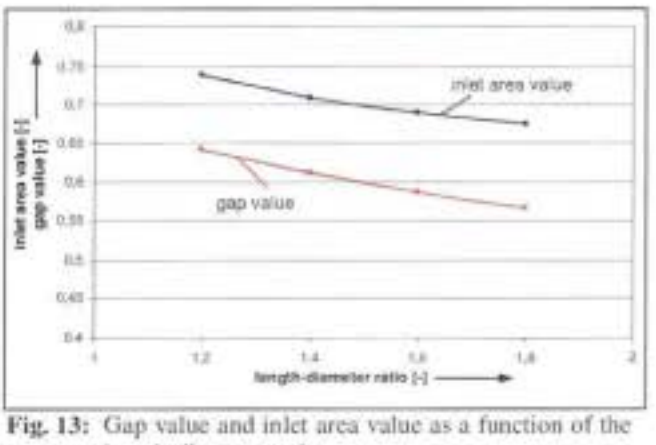

Fig. 13: Gap value and inlet area value as a function of the length-diameter ratio
($z_{MR} = 4$, $z_{FR} = 6$, $\varphi_{MR} = 300°$, $v_i = 4$)

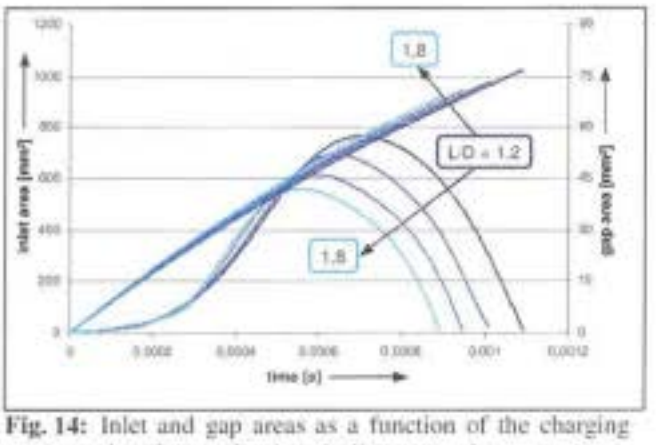

Fig. 14: Inlet and gap areas as a function of the charging time for varying length-diameter ratios
($z_{MR} = 4$, $z_{FR} = 6$, $\varphi_{MR} = 300°$, $v_i = 4$)

Energetic examination of variations in the length-diameter ratio

An examination of the inlet area and gap values permits conclusions to be drawn about the effect of varying the length-diameter ratio on the geometrical configuration of the inlet area and the gap situation. The relative importance of the dissipative effects of gap leakages and choke restriction has not yet been clarified. In an attempt to assess the opposing tendencies of the inlet area and gap values with reference to their effects on energy conversion efficiency, the internal efficiency rating and internal performance will be examined, as was already the case with variation of the wrap angle.

The efficiency rating for the charging process, and additionally for the charging process, expansion, and internal performance as a function of the length-diameter ratio are represented in **Fig. 15**.

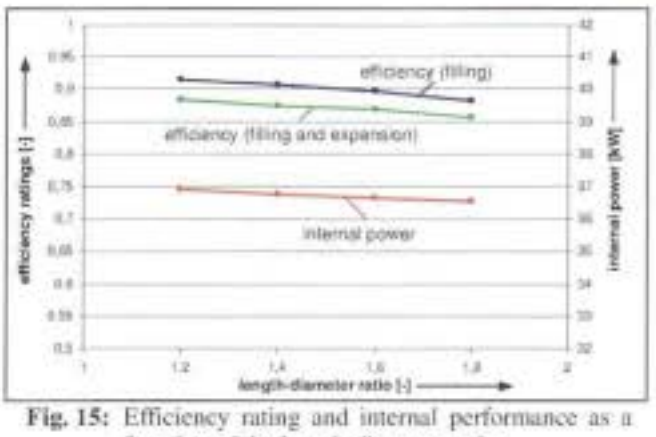

Fig. 15: Efficiency rating and internal performance as a function of the length-diameter ratio
($z_{MR} = 4$, $z_{FR} = 6$, $v_i = 4$, $L/D = 1.4$)

The best efficiency ratings are achieved by motors with small length-diameter ratios. Machines of this type profit, from an energetic point of view, from the long charging phases and the favourable geometry of the inlet area. As the length-diameter ratio increases, charging times become shorter, and inlet areas are reduced to an extent which cannot be compensated for by the improving gap situation. For motors of this type, less favourable efficiency ratings are the result. In contrast to an examination of wrap angles, gap masses which flow into the chambers during expansion do not seem to have a significant effect on the efficiency rating and energy conversion qualities of the machine. A tendency similar to that noted for the efficiency rating is exhibited by the internal performance of the machines being analysed. This drops continuously as the length-diameter ratio increases. As far as relative priorities among the loss mechanisms are concerned, the energetic examination of the length-diameter ratio reveals the special significance of the inlet area geometry and the charging time. Another similarity exists in connection with the wrap angle findings: the simulation results for varying length-diameter ratios justify the statement that in the parameter area under examination, a favourable inlet situation is always to be preferred to a favourable gap situation.

5. Conclusions

In the foregoing article the influence of geometrical machine parameters on the energy conversion efficiency of steam-powered screw motors has been examined. The variation parameters deployed were the internal volume ratio, the wrap angle and the

L	m	rotor length	#	gap / clearance
$\dot{m}$	$kg\,s^{-1}$	mass flow	HP	high pressure
n	s^{-1}	r.p.m	i	inner / internal
p	Pa	pressure	ia	inlet area
P	W	power / performance	id	ideal
R	$J\,kg^{-1}\,K^{-1}$	specific gas constant	max	maximum
t	s	time	MR	male rotor
T	K	temperature	LP	low pressure
u	$m\,s^{-1}$	rim speed	start	start of charging
			th	theoretical
			th,ex	theoretical start of expansion